***Manuscript, Table, and Figures**

Running title: paleo-SST in the equatorial Pacific

Spatial and temporal sea-surface temperatures in the eastern equatorial Pacific over the past 150 kyr

Keiji Horikawa[1,*], Masao Minagawa[1], Masafumi Murayama[2], Yoshihisa Kato[3], and Hirofumi Asahi[2]

[1]*Graduate School of Environmental Earth Science, Hokkaido University, Sapporo 060-0810, Japan*

[2]*Center for Advanced Marine Core Research, Kochi University, Japan*

[3]*School of Marine Science and Technology, Tokai University, Japan*

*Corresponding author; e-mail: horikawa@ees.hokudai.ac.jp

Abstract

We present the new alkenone-based sea-surface temperature (SST) records from the eastern equatorial Pacific over the past 150 kyr. Core HY04 (4ºN) at the North Equatorial Countercurrent (NECC) registered the invariant SSTs (25.8–27.2 ºC), whereas core HY06 (0ºN) registered cyclic glacial-interglacial SST variations (22.4–26.1 ºC). Although HY06 alkenone-based SST evolution was almost consistent with the previously published SST records from around the equator, at site HY04 alkenone- and foraminiferal Mg/Ca-based SSTs showed a large difference in the magnitude of LGM SST cooling. We hypothesize that alkenone-based SSTs might not fully express the true magnitude of glacial SST cooling in the NECC, as suggested by the coincidence of higher glacial productivity and unchanged glacial SSTs at site HY04. However, further SST data in the NECC are needed before this can be accepted with any degree of confidence.

1. Introduction

The eastern equatorial Pacific (EEP) is an important region within the framework of global climate changes. The coupled ocean-atmosphere circulation in the EEP affects the marine carbon and nitrogen cycles in the region significantly, and could have affected extratropical climate changes on glacial-interglacial timescales [e.g., *Cane*, 1998; *Chavez et al.,* 1999]. Ocean-atmosphere circulation in the EEP is strongly associated with the sea-surface temperature (SST) distribution; therefore, seasonal SST distribution in the EEP is influenced by the seasonal meridional shift of the Intertropical Convergence Zone (ITCZ) [*Mitchell and Wallace*, 1992]. Hence, it was considered that the reconstruction of spatial and temporal SST variations over glacial-interglacial cycles could provide foundational knowledge concerning past atmospheric conditions in the EEP [*Koutavas and Lynch-Stieglitz*, 2003]. However, the nature of spatial and temporal changes in the SST over the glacial-interglacial cycles in the EEP has not yet been completely clarified because various SST proxies exhibit different variability and most of SST records are within the cold tongue region [e.g., *Pisias and Mix,* 1997; *Koutavas et al.,* 2002]. This study present alkenone-based SST records from across the cold tongue, which will help to improve our understanding of past ocean-atmospheric conditions in the EEP.

2. Materials and Methods

Three piston cores–KH03-1 HY04 (4ºN), HY06 (0ºN), and HY08B (6ºS)–were collected along the 95ºW transect of the EEP during the *R/V Hakuho-Maru* cruise (Fig. 1). The age models for KH03-1 cores were based on the planktonic foraminifera *Globigerinoides ruber*

(250–355 μm fraction) $\delta^{18}O$ records and AMS-^{14}C ages of foraminiferal tests (*Neogloboquadrina dutertrei*), applying the SPECMAP $\delta^{18}O$ chronology [*Martinson et al*., 1987] (Table. 1). The sedimentation rates were 0.9–3.4 cm/kyr for HY04 and 1.6–21 cm/kyr for HY06. The high sedimentation rate of 21 cm/kyr corresponds to the period of 19–20 ka determined by AMS-^{14}C ages. For HY08B, $\delta^{18}O$ chronology has not yet been established, but two AMS-^{14}C ages exhibit a horizon during the last glacial maximum (LGM) and sedimentation rates of less than 2.0 cm/kyr. The AMS-^{14}C ages are intercalated in marine isotope stage (MIS) 2, and thus, the present age models might not influence the estimations of the SST difference between the late Holocene and the LGM significantly (Fig. 1).

Each sediment sample (thickness: 2.5 cm) was taken at intervals of 2.5–5.0 cm. The lipids of each sample were extracted from dry sediments (1–3 g) by an accelerated solvent extractor (ASE-200, Dionex Japan, Ltd) using a mixture of dichloromethane and methanol (6/4 v/v) as a solvent. Alkenones were separated from the neutral compounds by silica gel column chromatography and quantified by gas chromatography with flame-ionization detection [*Yamamoto et al*., 2000]. Alkenones are produced by a few species of haptophyte algae that live in the near-surface [e.g., *Volkman et al.,* 1995]. Therefore, SST can be estimated from the relative abundance of C_{37} unsaturated alkenones ($U^{k'}_{37}$ index) and the laboratory culture relationship between $U^{k'}_{37}$ and SST ($U^{k'}_{37} = 0.034 \times SST + 0.039$) [*Prahl et al*., 1988]. Replicate analyses of a standard EEP sediment indicated a standard deviation of 0.14 ºC (n = 4) in $U^{k'}_{37}$ estimates in our procedure.

Based on the equation [*Prahl et al.,* 1988], the alkenone-based SSTs of the uppermost portions of the Holocene samples from cores HY04 and HY06 showed the annual mean SSTs (0–10 m) [*Levitus and Boyer,* 1994]. Thus, we equate the alkenone-based SST from cores HY04 and HY06 with mean annual SST. In contrast, the alkenone-based SST of the uppermost portions of core HY08B was lower than the annual mean SST by 2 ºC, implying a seasonal bias in the SSTs recorded during the upwelling seasons at this site.

3. Results

The cold tongue region in the EEP is characterized by a series of nearly zonal currents, with the temperature decreasing gradually from the north to south (Fig. 1). Core HY04–recovered from the warm-water NECC–showed fewer variations in SSTs (n = 51, 25.8–27.2 ºC), whereas core HY06–recovered at the equator–showed cyclic glacial-interglacial SST variations (n = 84, 22.4–26.1 ºC) (Fig. 2). The alkenone-based SST records from different zonal currents exhibited different temporal trends over the past 150 kyr. Further, HY04 SSTs were observed to be 26.2 ± 0.03 ºC during the LGM (19–23 ka; n=3) and 26.5 ºC during the early Holocene (10 ka). At this site, SST cooling during the LGM relative to the present mean annual SST (27 ºC) could be estimated to be 0.8 ºC. The SST data from the uppermost portion of core HY04 is missing due to low concentration of alkenone, but alkenone concentration in the remaining portions of core HY04 was sufficient to obtain SST data. The SSTs recorded for core HY06 during the LGM (19–23 ka; n = 10) are 22.9 ± 0.4 ºC and during the late Holocene (0–5 ka; n = 5), 24.3 ± 0.4 ºC, indicating an average SST difference of 1.4 ºC between the LGM and the late Holocene. For core HY08B, although the number of alkenone-based SST records was limited, the amplitude observed was 23.8–25.6 ºC for the past ~30 kyr. The LGM horizon determined by AMS-^{14}C ages (23 ka) was 23.8 ºC. If this SST estimate at 23 ka is assumed to be the mean annual SST, the LGM SST cooling relative to the present (24.3 ºC) is 0.5 ºC.

4. Discussion and Conclusion

The new alkenone-based SST evolution from site HY06 (0ºN) resembles the alkenone-based SST record (ODP 846, 3ºS) over the past 150 kyr [*Liu and Herbert,* 2004]; both exhibit the following two characteristics: (1) monotonic decrease from ~50 ka to the early MIS 2 and (2) warmer SSTs during MIS 6 than those during the LGM (Fig. 2). These SST patterns have also been observed in the subantarctic waters off eastern New Zealand [*Pahnke and Sachs,* 2006]. Given that the subsurface water in the EEP originates mainly from the high and mid-latitudes of the South Pacific [*Toggweiler et al.,* 1991], it is possible that the temperature of the EEP subsurface water is influenced by the SSTs of the subantarctic waters [*Liu and Herbert,* 2004]. The ocean-atmosphere model indicates that the extratropical SST changes will affect ocean-atmospheric conditions in tropics through atmospheric bridge and thermocline ventilation [*Yang and Liu,* 2005]; this supports that the EEP SST evolution could be partly controlled by remote SST forcing in the subantarctic waters.

However, we suppose that the influence of precessional orbital forcing might be importance in the low-latitudes, as documented from several low-latitude climate records [e.g., *Perks et al.,* 2002; *Cruz et al.,* 2005], though greenhouse forcing is also hypothesized to influence low-latitude climate system [*Lea*, 2004]. In the EEP, we found that the responses of the ocean-atmospheric conditions to the precessional insolation changes are clearly documented in the cold tongue based on the SST gradient between sites HY06 and TR163-19 (Mg/Ca-based SST) [*Lea et al.,* 2000], though the SSTs were derived from different SST proxies. The SST gradient (MIS 2, 4, 5b, early MIS 5d, and 6) registered a decrease during the periods of increased southern (decreased northern) hemisphere summer insolation (Fig. 2). If the temporal changes in the SST gradient are not a result of artifacts due to different SST proxies and/or age model uncertainty but a true signal generated as a response to the precessional forcing, we can conclude that the temporal changes in the cold tongue SST gradient are imprinted by seasonal variations in the precession-modulated trade wind field. However, whether the SST distribution in the cold tongue and in more widely spaced regions has changed systematically in response to the precessional insolation cycles still remains unresolved [e.g., *Koutavas et al.,* 2002; *Lea et al.,* 2006].

First, we assumed that it might be better to investigate the SST gradient across the ITCZ-cold tongue between sites HY04 and HY06 to observe the dynamics of the cold tongue in response to the precessional insolation cycles. However, at this stage, we hesitate to discuss the temporal changes in the alkenone-based SST gradient between the two sites because as discussed below, there is a concern whether HY04 alkenone-SSTs follow the mean annual SST during cold periods.

HY04 alkenone-based SSTs show minor variability in the NECC during the last glacial-interglacial cycle (Fig. 2). Similar to the case of HY04 alkenone-based SSTs, the SSTs inferred from planktonic foraminiferal assemblages also show low variability in the NECC over the past 35 kyr [*Martínez et al.,* 2003] (Fig. 1). If the SSTs with low variability hold true in the NECC region, then it is possible that these sites might have been influenced by the oligotrophic, warm NECC throughout the last glacial-interglacial cycle. However, the alkenone abundance in core HY04, which could be indicative of a productivity change due to a good correlation with total organic carbon (TOC) content ($r = 0.48$), exhibits a steady increase during the cold periods (MIS 2, 4, 5b, and 6) (Fig. 2). Assuming that the alkenone abundance in the sediments is indicative of alkenone flux from the euphotic zone, the increased alkenone abundance during the cold periods requires higher fluxes of nutrients and micronutrients to the euphotic zone. If so, it seems unlikely that site HY04 is covered by the NECC even during the cold periods.

Sedimentary $\delta^{15}N$ of HY04 shows lower glacial values and an inverse relationship with alkenone abundance [*Horikawa et al.,* in preparation]. The result agrees with the lower LGM $\delta^{15}N$ and higher LGM TOC (wt%) records in the Panama basin that are considered to be due to enhanced vertical mixing during the LGM [*Farrell et al.,* 1995]. Therefore, we suppose that site HY04 experienced enhanced vertical mixing during the LGM. We are unable to discuss quantitatively the issue of how much SST cooling is sufficient to explain the observed increase in productivity during the LGM. However, at site HY06 where the Equatorial Undercurrent (EUC) feeds nutrients directly to the surface, the increases in alkenone and TOC (wt%) in response to 1.4 ºC of LGM SST cooling were lower than the productivity increases at site HY04 indicating 0.8 ºC of LGM SST cooling. Sedimentary organic matter content from each site cannot be completely compared because of the affect of sedimentation rates and sedimentary environments [e.g., *Arthur et al.,* 1998]; however, we suppose that the higher glacial productivities at site HY04 and in the Panama Basin [*Farrel et al.,* 1995; *Loubere*, 2002] require a greater decrease in the SST than 1.4 ºC observed at site HY06.

Further, a concern regarding the possible underestimation of the glacial SST cooling at site HY04 is suggested by the foraminiferal Mg/Ca-based SSTs (*G. ruber*) recorded during the LGM. Mg/Ca-based SST in core HY04 shows a cooling of ~3 ºC (n = 2) during the LGM [*Asahi et al.,* in preparation]. The estimation is consistent with the LGM SST cooling at 2ºN–3ºN (2.8–3.3 ºC) [*Lea et al.,* 2000; *Koutavas and Lynch-Stieglitz*, 2003], but shows a difference in the magnitude of LGM SST cooling compared to the alkenone-based SSTs. Similar differences in the two SST proxies are often reported [e.g., *Nürnberg et al.,* 2000], and are usually explained by invoking differences in the water column and/or seasonal temperatures reflected by the proxies [*Brown and Yoder,* 1994], or differences in sensitivity to other environmental factors (e.g., nutrient and light [*Prahl et al.,* 2006]). Although we do not have a plausible explanation for the discrepancy in core HY04 at this stage, the lower Mg/Ca-based SST estimates, the higher productivity, and the lower $\delta^{15}N$ at HY04 during the LGM suggest that alkenone-based SSTs might not fully express the LGM SST cooling that the site experiences.

If the HY04 Mg/Ca-based SSTs are indicative of the decrease in the mean annual SST during the LGM, the SST gradient across the cold tongue (HY04–HY06) decreases during the LGM. This data implies that the SST distribution across the cold tongue has changed systematically in response to the precessional insolation cycles, as observed from the changes in the SST difference between HY06 and TR163-19 (Fig. 2). However, if HY04 alkenone-based SSTs are indicative of the mean annual SST recorded during the LGM, then the SST gradient (HY04–HY06) is steeper during the LGM than in the warm periods. If this is true, the systematic changes in the SST gradient between sites HY06 and TR163-19 are not supported by the alkenone-based SST gradient across the ITCZ-cold tongue. Furthermore, if the warmer, fresher waters of the NECC persisted during the LGM, the northeasterly trade winds and the associated NEC might have weakened, and the cross-equatorial water-mass exchanges might have been limited due to the distinct north-south salinity gradient [*Andreasen et al.,* 2001]. However, these oceanographic conditions make it difficult to explain the higher LGM productivity observed in the Panama Basin [e.g., *Loubere*, 2002].

The glacial SST in the NECC is a crucial component for discussing past ocean-atmospheric conditions in the EEP, but we have not yet known the true magnitude of glacial SST cooling.

Therefore, we must carefully clarify the degree of glacial SST cooling by applying multiple-SST proxies in future studies.

Acknowledgments

We are thankful to M. Shigemitsu and P. Rafter for their valuable comments and an anonymous reviewer and Zhonghui Liu for their constructive comments on earlier versions of this paper. We would also like to thank T. Herbert for kindly providing access to unpublished data. This work was supported by a research fellowship of JSPS for young scientists to K.H (No. 15050041) and by 21st Century COE Program (E-01) and Grant-in-Aid for Science Research (No. 16201001) of MEXT.

References

Andreasen, D. H., A. C. Ravelo, and A. J. Broccoli (2001), Remote forcing at the Last Glacial Maximum in the tropical Pacific Ocean, *J. Geophys. Res., 106,* 879–897.

Arthur, M. A., W. E. Dean, and K. Laarkamp (1998), Organic carbon accumulation and preservation in surface sediments on the Peru margin, *Chem. Geol., 152,* 273–286.

Bard, E. (1988), Correlation of accelerator mass spectrometry ^{14}C ages measured in planktonic foraminifera: Paleoceanographic implications, *Paleoceanography, 3*, 635–645.

Bard, E. (1998), Geochemical and geophysical implications of the radiocarbon calibration, *Geochim. Cosmochim. Acta, 62*, 2025–2038.

Berger, A., and M. F. Loutre (1991), Insolation values for the climate of the last 10 million years, *Quat. Sci. Rev., 10,* 297–317.

Brown, C. W., and J. A. Yoder (1994), Coccolithophorid blooms in the global ocean, *J.*

Geophys. Res., 99, 7467–7482.

Cane, M. (1998), A role for tropical Pacific, *Science, 282,* 59–61.

Chavez, F. P., P. G. Strutton, G. F. Friederich, R. A. Feely, G. C. Feldman, D. G. Foley, and M. J. McPhaden (1999), Biological and chemical response of the equatorial Pacific Ocean to the 1997-98 El Niño, *Science, 286*, 2126–2131.

Cruz, F. W., S. J. Burns, I. Karmann, W. D. Sharp, M. Vuille, A. O. Cardoso, J. A. Ferrari, P. L. S. Dias, and O. Viana (2005), Insolation driven changes in atmospheric circulation over the past 116,000 years in subtropical Brazil, *Nature, 434,* 63–66.

Farrell, J. W., T. F. Pedersen, S. E. Calvert, and B. Nielsen (1995), Glacial-interglacial changes in nutrient utilization in the equatorial Pacific Ocean, *Nature, 377,* 514–517.

Koutavas, A., J. Lynch-Steiglitz, T. M. J. Marchitto, and J. P. Sachs (2002), El Niño-like pattern in ice age tropical Pacific sea surface temperature, *Science, 297*, 226–230.

Koutavas, A., and J. Lynch-Stieglitz (2003), Glacial-interglacial dynamics of the eastern equatorial Pacific cold tongue-Intertropical Convergence Zone system reconstructed from oxygen isotope records, *Paleoceanography, 18(4),* 1089, doi:10.1029/2003PA000894.

Lea, D. W. (2004), The 100 000-yr cycle in tropical SST, greenhouse forcing, and climate sensitivity, *J. Climate, 17,* 2170–2179.

Lea, D. W., D. K. Pak, and H. J. Spero (2000), Climate impact of late Quaternary equatorial Pacific sea surface temperature variations, *Science, 289*, 1719–1724.

Lea, D. W., D. K. Pak, C. L. Belanger, H. J. Spero, M. A. Hall, and N. J. Shackleton (2006), Paleoclimate history of Galapagos surface waters over the last 135,000 yr, *Quat. Sci. Rev.,* (in press).

Levitus, S., and T. Boyer (1994), *World Ocean Atlas 1994*, vol. 4, *Temperature*, *NOAA Atlas*

NESDIS 4, U.S. Dep. of Commer., Washington, D.C.

Liu, Z., and T. D. Herbert (2004), High-latitude influcence on the eastern equatorial Pacific climate in the early Pleistocene epoch, *Nature, 427*, 720–723.

Loubere, P. (2002), Remote vs. local control of changes in eastern equatorial Pacific bioproductivity from the last glacial maximum to the present, *Global Planet. Change, 35,* 113–126.

Martínez, I., L. Keigwin, T. T. Barrows, Y. Yokoyama, and J. Southon (2003), La Nina-like conditions in the eastern equatorial Pacific and a stronger Choco jet in the northern Andes during the last glaciation, *Paleocoeanography, 18(2)*, 1033, doi:10.1029/2002PA000877.

Martinson, D. G., N. G. Pisias, J. D. Hays, J. Imbrie, T. C. Moore, Jr, and N. J. Shackleton (1987), Age dating and the orbital theory of the ice ages: development of a high-resolution 0 to 300,000-year chronostratigraphy, *Quat. Res., 27*, 1–29.

Mitchell, T. P., and J. M. Wallace (1992), The annual cycle in equatorial convection and sea-surface temperature, *J. Climate, 5*, 1140–1156.

Nürnberg, D., A. Müller, and R. Schneider (2000), Paleo-sea surface temperature calculations in the equatorial east Atlantic from Mg/Ca ratios in planktic foraminifera: A comparison to sea surface temperature estimates from $U^{k'}_{37}$, oxygen isotopes, and foraminiferal transfer function, *Paleoceanography, 15,* 124–134.

Pahnke, K., and J. P. Sachs (2006), Sea surface temperatures of southern midlatitudes 0–160 kyr B.P., *Paleoceanography, 21,* PA2003, doi:10.1029/2005PA001191.

Perks, H. M., C. D. Charles, and R. F. Keeling (2002), Precessionally forced productivity variations across the equatorial Pacific, *Paleoceanography, 17(3),* 1037, doi:10.1029/ 2000PA000603.

Pisias, N. G., and A. C. Mix (1997), Spatial and temporal oceanographic variability of the eastern equatorial Pacific during the late Pleistocene: Evidence from radiolaria microfossils, *Paleoceanography, 12*, 381– 393.

Prahl, F. G., L. A. Muelhausen, and D. L. Zahnle (1988), Further evaluation of long-chain alkenones as indicators of paleoceanography conditions, *Geochim. Cosmochim. Acta, 52*, 2303–2310.

Prahl, F. G., A. C. Mix, and M. A. Sparrow (2006), Alkenone paleothermometry: Biological lessons from marine sediment records off western South America, *Geochim. Cosmochim. Acta, 70*, 101–117.

Stuiver, M., and P. J. Reimer (1993), Extended ^{14}C data base and revised CALIB 3.0 ^{14}C age calibration program, *Radiocarbon, 35,* 15–230.

Toggweiler, J., D. Dixon, and W. S. Broecker (1991), The Peru upwelling and the ventilation of the South Pacific thermocline, *J. Geophys. Res., 96*, 20,467–20,497.

Volkman, J. K., S. Barret, S. I. Blackburn, and E. L. Sikes (1995), Alkenones in *Geophyrocapsa oceanica*: implications for studies of paleoclimate, *Geochim. Cosmochim. Acta, 59*, 513–520.

Yamamoto, M., M. Yamamuro, and R. Tada (2000), Late Quaternary records of organic carbon, calcium carbonate and biomarkers from Site 1016 off Point Conception, California margin, *Proc. ODP Sci. Res., 167*, 183–194.

Yang, H., and Z. Liu (2005), Tropical-extratropical climate interaction as revealed in idealized coupled climate model experiments, *Climate Dynamics, 24,* 863–879.

Captions

Table. 1. Core locations and ^{14}C ages for the sediment cores. We used 400 years as a reservoir age of carbon in the ocean [*Bard*, 1988]. Radiocarbon ages were converted to calendar ages using the CALIB5.0 [*Stuiver and Reimer,* 1993] or *Bard* [1998].

Figure 1. Plot of mean annual SST (ºC) [*Levitus and Boyer,* 1994] with the amount of estimated cooling during the LGM at each core site compared to the late Holocene (or mean annual SST). Major oceanic currents in the EEP are the North and South Equatorial Currents (NEC and SEC), and their countercurrents (NECC and SECC), and Equatorial Undercurrent (EUC). Shaded values indicate alkenone-based SST estimate. SST data are from *Martínez et al.* [2003] for core TR163-11 (star; based on faunal proxies), *Liu and Herbert* [2004] for ODP 846, *Lea et al.* [2000] for TR163-19.

Figure 2. Comparison of four SST records in the EEP with the 15ºS January insolation changes [*Berger and Loutre*, 1991] over the 150 kyr. Top panel shows planktonic foraminifera $\delta^{18}O$ records from cores HY04 and HY06, together with AMS-^{14}C age-control points (circles and squares are for HY04 and HY06). HY04 alkenone abundance is also indicated. ODP 846 alkenone-SST is from *Liu and Herbert* [2004]. Normalized SST difference between HY06 alkenone-SST and TR163-19 Mg/Ca-SST [*Lea et al.,* 2000] is well correlated to the precessional insolation changes.

Site	Latitude	Longitude	Depth	Core length
HY04	**4º01.66'N**	**95º03.45'W**	**3563 (m)**	**12.3 (m)**
	depth (cm)	^{14}C age (yr BP)	calendar calibrated age (yr BP)	calibration
	8.5	4381 ± 27	4497	Calib 5.0
	18.2	8559 ± 35	9076	Calib 5.0
	37.6	15408 ± 60	18247	Calib 5.0
	57	22192 ± 77	25667	Bard, 1998
	69.2	25359 ± 100	29305	Bard, 1998
HY06	**0º01.52'N**	**95º26.52'W**	**3242 (m)**	**14.2 (m)**
	depth (cm)	^{14}C age (yr BP)	calendar calibrated age (yr BP)	calibration
	11.1	3465 ± 26	3299	Calib 5.0
	28.5	10409 ± 39	11447	Calib 5.0
	63.7	16593 ± 55	19385	Calib 5.0
	86.1	17754 ± 60	20470	Calib 5.0
HY08B	**5º57.49'S**	**94º55.85'W**	**3867 (m)**	**13.7 (m)**
	depth (cm)	^{14}C age (yr BP)	calendar calibrated age (yr BP)	calibration
	28.6	19517 ± 68	22588	Calib 5.0
	41.1	26110 ± 102	30159	Bard, 1998

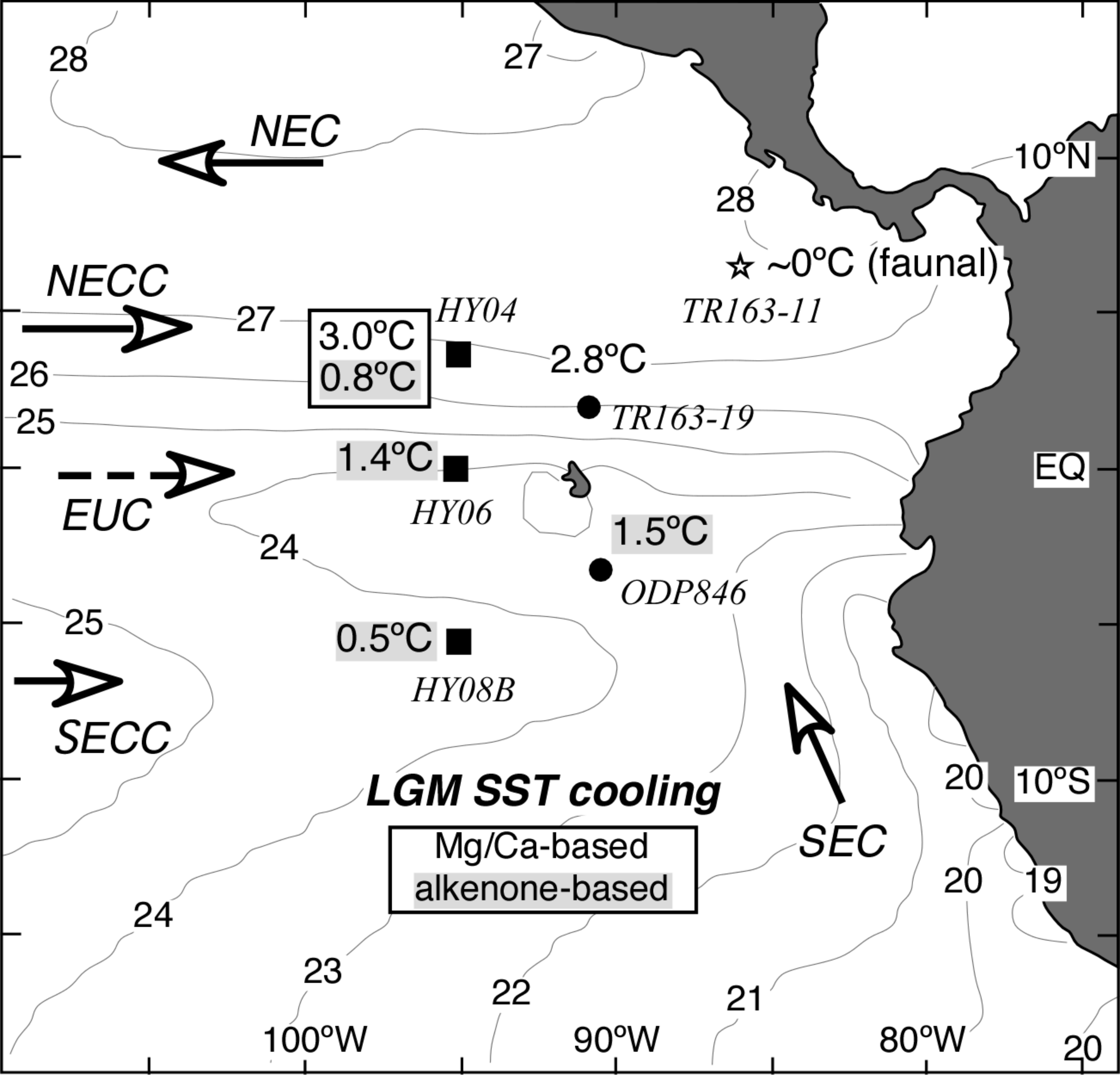

28
27
NEC
10ºN
28
☆ ~0ºC (faunal)
NECC
TR163-11
27
HY04
3.0ºC
0.8ºC
2.8ºC
26
25
TR163-19
1.4ºC
EQ
EUC
HY06
1.5ºC
24
ODP846
25
0.5ºC
HY08B
SECC
LGM SST cooling
20
10ºS
Mg/Ca-based
alkenone-based
SEC
20
19
24
23
22
21
100ºW
90ºW
80ºW
20

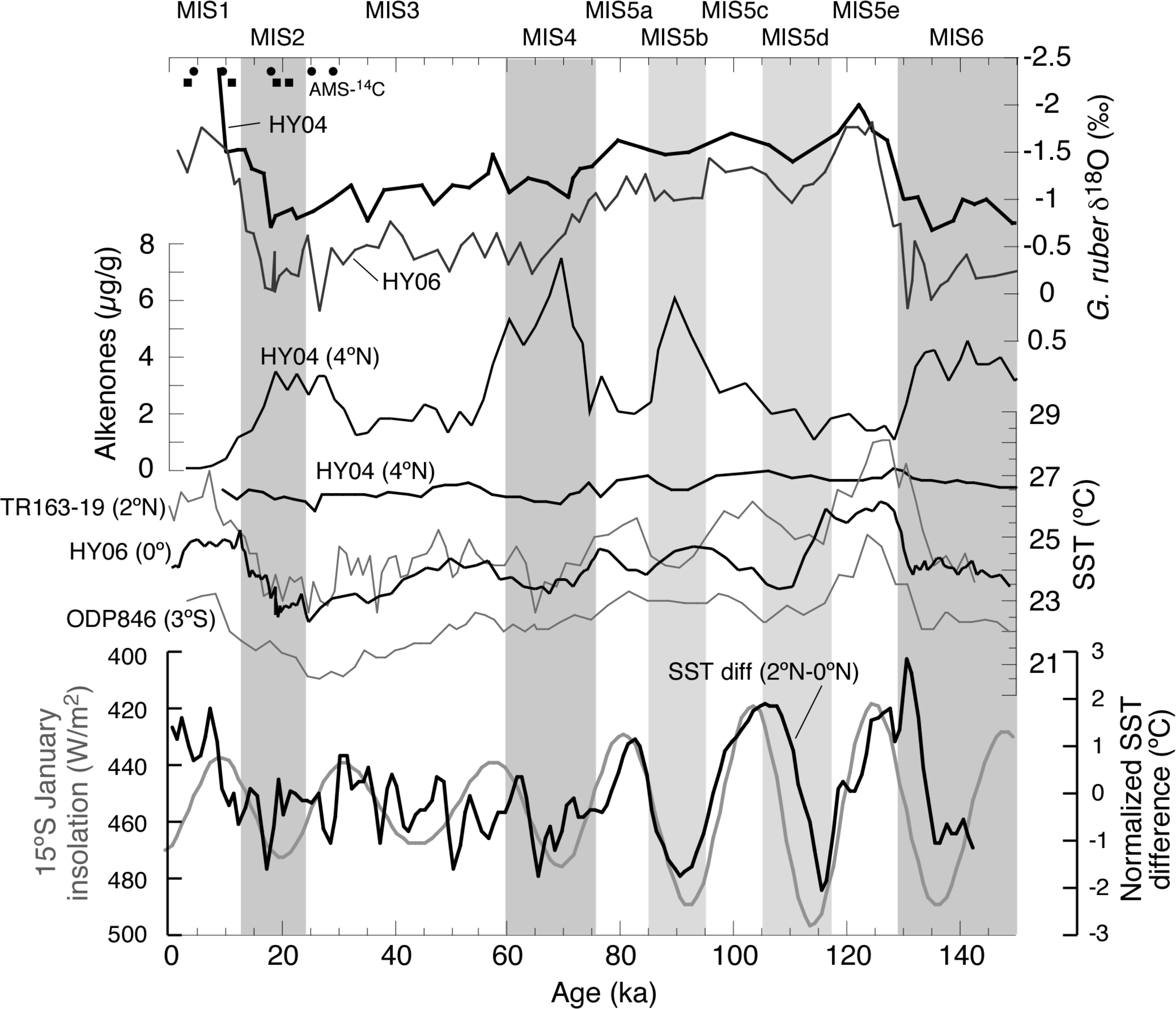

MIS1
MIS2
MIS3
MIS4
MIS5a
MIS5b
MIS5c
MIS5d
MIS5e
MIS6
AMS-14C
HY04
HY06
G. ruber δ18O (‰)
Alkenones (μg/g)
HY04 (4ºN)
HY04 (4ºN)
TR163-19 (2ºN)
HY06 (0º)
ODP846 (3ºS)
SST (ºC)
SST diff (2ºN-0ºN)
15ºS January insolation (W/m2)
Normalized SST difference (ºC)
Age (ka)